Magnetic shielding of a thin Al/steel/Al composite

Paul Clérico, Xavier Mininger, Laurent Prevond, Thierry Baudin, Anne-Laure Helbert

Magnetic shielding of a thin Al/steel/Al composite

Paul Clérico, Xavier Mininger, Laurent Prevond, Thierry Baudin, Anne-Laure Helbert

Magnetic shielding of a thin Al/steel/Al composite

Paul Clérico
Université Paris-Saclay, CNRS, Institut de Chimie Moléculaire et des Matériaux d'Orsay, Orsay, France; Université Paris-Saclay, CentraleSupélec, CNRS, Laboratoire de Génie Electrique et Electronique de Paris, Gif-sur-Yvette, France; Sorbonne Université, CNRS, Laboratoire de Génie Electrique et Electronique de Paris, Paris, France and SATIE – CNAM, Conservatoire National des Arts et Métiers, Paris, France

Xavier Mininger
Université Paris-Saclay, CentraleSupélec, CNRS, Laboratoire de Génie Electrique et Electronique de Paris, Gif-sur-Yvette, France and Sorbonne Université, CNRS, Laboratoire de Génie Electrique et Electronique de Paris, Paris, France

Laurent Prévond
SATIE – CNAM, Conservatoire National des Arts et Métiers, Paris, France, and

Thierry Baudin and Anne-Laure Helbert
Université Paris-Saclay, CNRS, Institut de Chimie Moléculaire et des Matériaux d'Orsay, Orsay, France

Received 30 September 2019
Revised 11 December 2019
7 February 2020
Accepted 13 March 2020

Abstract

Purpose – This paper aims to investigate the efficiency of a laminated composite for shielding applications. The solution has to be efficient not only for the shield against static magnetic fields but also "for low-frequency ones, in order to be well-suited for applications with electromagnetic perturbations in the frequency range DC to 100 kHz."

Design/methodology/approach – The composite constituted of a steel sheet taken in a sandwich between two aluminum (Al) sheets is produced by cold roll bonding. A good adherence between Al and steel sheets, ensuring a good mechanical resistance, is obtained with a specific process. A previous study has shown that the optimal trade-off between adherence and magnetic shielding effectiveness (SE_H) is obtained with a 230 μm composite produced with an initial thickness of Al and steel sheets, respectively, of 250 and 100 μm. In this paper, the 230 μm Al/steel/Al composite is used in three applications modelized by two-dimensional numerical simulations. To obtain reasonable computation time for the simulations, a homogenization method is applied to the composite. Studied applications are a cylindrical box containing a coil, a square box under an external magnetic field and a high voltage cable.

Findings – In each application, SE_H is calculated at low frequency and different materials (Al/steel/Al, Al, steel and copper) are compared. It is observed that, in each application, the composite presents higher SE_H at equal mass, especially for frequencies between 5 and 100 kHz.

This work is supported by a public grant overseen by the French National Research Agency (ANR) as part of the "Investissement d'Avenir" program, through the "IDI 2016" project funded by the IDEX Paris-Saclay, ANR-11-IDEX-0003-02.

Originality/value – The proposed approach, from the material point of view to the system consideration, shows that the thin bimetallic composite is an innovative and promising solution for magnetic shielding in the case of applications with both DC and low-frequency perturbations.

Keywords Numerical analysis, Finite element method, Homogenization method, Magnetic shielding

Paper type Research paper

1. Introduction

Electromagnetic pollution is a source of disturbance for sensitive electrical and electronic devices (Smolenski *et al.*, 2014) and can be potentially harmful to human beings (Dawson *et al.*, 2002). Then, living and critical components have to be protected from electric and magnetic fields, and electronic devices have to confine these fields thanks to electromagnetic shielding (Abdelli *et al.*, 2012; Ahn *et al.*, 2010).

Common materials used for electromagnetic shields are metals (Liu *et al.*, 2017; Xu and Hao, 2014) and carbons (Chung, 2001; Li *et al.*, 2018). Lightweight materials, required in the transportation industry, composed of metal or carbon-reinforced polymer have been greatly studied (Al-Ghamdi *et al.*, 2015; Ray *et al.*, 2010). However, polymers are insulating, and reinforced polymer composites show lower electrical conductivity than bulk metal. Multi-layer composite is also an effective means to shield against electromagnetic fields (Ma *et al.*, 2016; Kim *et al.*, 2016).

Low-frequency magnetic fields can cause noise and disturbance to sensitive devices and are emitted, by instance, by electrical motors, power supplies and power converters. In this paper, the shielding effectiveness (SE_H) of a 230 μm Al/steel/Al composite with homogenized properties is studied and compared to aluminum (Al), steel and copper (Cu) ones in various applications modelized by the finite element method. The idea is to propose a solution that gives an efficient shielding against both static and low-frequency electromagnetic fields. Furthermore, the thin composite thickness ensures its lightness and flexibility and can be manually bent. Another main interesting advantage of this solution is that Al layers in the composite protect the steel layer from potential oxidation. Thus, the composite presents the advantage of being adapted to oxidizing atmospheres. In this paper, SE_H is studied for a magnetic field at low frequencies from 1 Hz to 100 kHz. Both experimental and numerical approaches, including the homogenization process, are used to present a global study, from the elaboration of the composite material to the shielding application.

2. Materials and applications

2.1 Aluminum/steel/aluminum composite

The studied composite is composed of one layer of steel sandwiched between two layers of Al. Commercial low-carbon steel DC01 and 8011-Al alloy are chosen as raw materials with,

Table I. Chemical compositions (Wt. per cent) of DC01 steel and 8011-Al alloy

%Al	%Fe	%Si	%Mn	%Zn	%Cu	%Ti	%Cr	%Mg
Al8011								
Bal	0.6-1	0.5-0.9	≤0.2	≤0.1	≤0.1	≤0.08	≤0.05	≤0.05
DC01								
	%Fe	%C	%Mn	%P	%S	%Si	%Al	
	Bal	≤0.12	≤0.6	≤0.045	≤0.045	≤0.03	≤0.02	

respectively, the initial thickness of 100 and 250 μm. DC01 steel is mainly used for drawing and forming applications. 8011-Al is a Fe and Si-based Al alloy, which is widely used in the industry. The chemical compositions of these two materials are listed in Table I.

The Al/steel/Al composite is produced by cold roll bonding (CRB) with different reduction rates equal to $1 - h_f/h_i$ with h_f and h_i, respectively, the final and initial thickness (Figure 1). Figure 1 presents a schematic diagram of the composite CRB following a rolling-normal cross-section.

In a previous study (Clérico *et al.*, 2019), the trade-off between SE_H and Al/steel interface adherence has been studied. The following part gives a summary that justifies the later thickness of the composite used for the considered applications.

Figure 2 shows the electronic bench used to measure the experimental SE_H of the composite. A sinusoidal current is produced by a low-frequency generator associated with a linear amplifier. The effective value of the current intensity is 2 A. A coil with a height of 18.5 mm, an inner and outer diameter of 15 and 30 mm generates a magnetic field. The latter is then

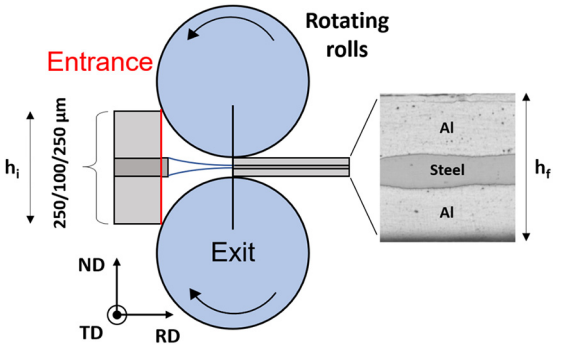

Figure 1.
CRB of Al/steel/Al composite

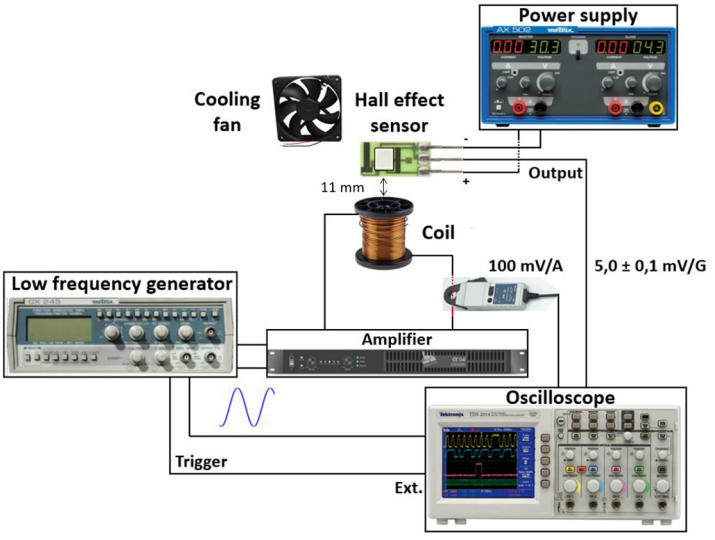

Figure 2.
Electronic bench scheme

measured 11 mm above the coil by a Hall effect sensor with a sensibility of (5.0 ± 0.1) mV/G. The SE_H of the composite is measured considering square samples placed 6 mm above the coil. A cooling fan is used to limit the temperature influence.

Figure 3 shows that the experimental SE_H of 3 × 3 cm^2 samples (square of 3 by 3 cm) measured at 1 and 10 kHz decreases, firstly, linearly due to the thickness reduction, and then continues to decrease with a steeper slope due to the steel fragmentation that occurred during the CRB. Indeed, the more the reduction rate increases, the more the steel fragmentation is present, leading to the decrease of the magnetic permeability of the tri-layer in the rolling direction (RD).

Figure 4 shows that the quality of the Al/steel interface adherence increases with the reduction rate. Adherence has been determined by the tensile bond strength (TBS) test that

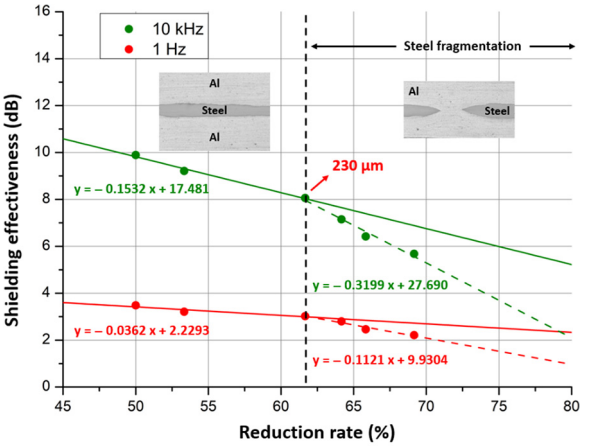

Source: Clérico *et al.* (2019)

Figure 3.
SE_H of 3 × 3 cm^2 tri-layer samples at different reduction rate measured experimentally

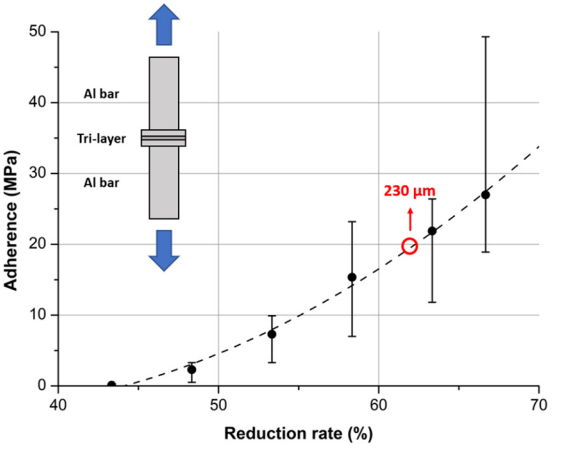

Source: Clérico *et al.* (2019)

Figure 4.
TBS of Al/Steel interfaces

gives for each reduction rate the tensile stress value at the interface rupture (TBS). This method is detailed in a previous paper (Clérico *et al.*, 2019).

The optimal trade-off between SE_H and adherence of Al/steel interfaces is then obtained with a 230 μm thickness composite. Indeed, the 230 μm composite shows very little steel fractures, that limit the negative effect on SE_H and give a good quality of adherence with a TBS around 19-20 MPa. In this case, Al and steel layer thicknesses of the composite considered in the numerical approach are then around 191.6 (2 × 95.8) and 38.4 μm, respectively.

2.2 Applications

In this paper, three applications are modelized in COMSOL Multiphysics with alternative current/direct current module and studied in the frequency range of 1 Hz-100 kHz: a cylindrical box containing a coil to simulate the confinement of a magnetic field, a squared box placed in an external magnetic field to simulate the protection of a sensitive component, and finally, a simplified model of a high voltage cable, that is closer to actual industrial applications. Figures 5-7 show the modelized geometries of the three applications.

The cylindrical box is modelized with a two-dimensional axisymmetric model. The box has a diameter and a height of 50 mm. In this first approach, the coil is considered centered inside the cylindrical box. To simulate the magnetic field, an effective current of 2 A,

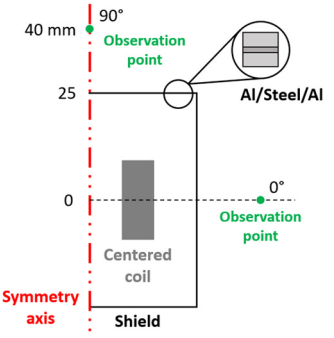

Note: SE_H observation points are indicated

Figure 5.
Cylindrical shielding box (50 × 50 mm) containing a coil (two-dimensional-axis)

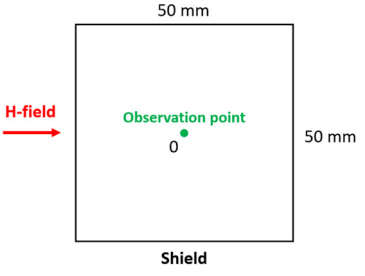

Note: SE_H observation point is indicated

Figure 6.
Square shielding box (50 × 50 mm) under an external *H*-field (two-dimensional)

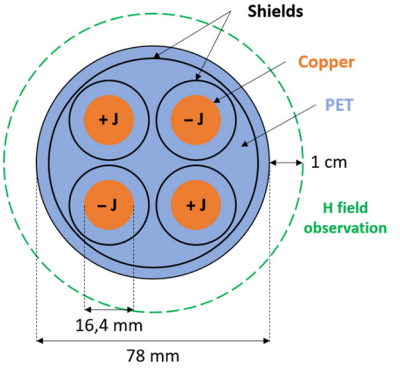

Figure 7.
Simplified model of a high voltage cable (two-dimensional)

Note: SE_H observation points are indicated

corresponding to a current density of around 1.44e6 A/m^2, is considered. The SE_H of this box is studied at two points, with horizontal and vertical locations, both placed at 15 mm of the shield. This first application simulates the magnetic shielding in near-field condition.

The squared box is modelized with a two-dimensional plane model. The box has a side of 50 mm and is placed in an external magnetic field obtained with magnetic vector boundary condition ($n \times A = n \times A_0$). The SE_H is studied at the center of the box. This second application simulates the magnetic shielding in far-field condition.

The high voltage cable is also modelized with a two-dimensional plane model. The simplified geometry (Figure 7) has been inspired by the work of Nguyen (2013). Figure 8 shows the actual geometry of the high voltage cable studied by Nguyen (2013). In a high voltage cable, perturbations and proximity effects between conductors can take place, affecting the cable integrity and leading to malfunctions. An adapted shielding can prevent these perturbations.

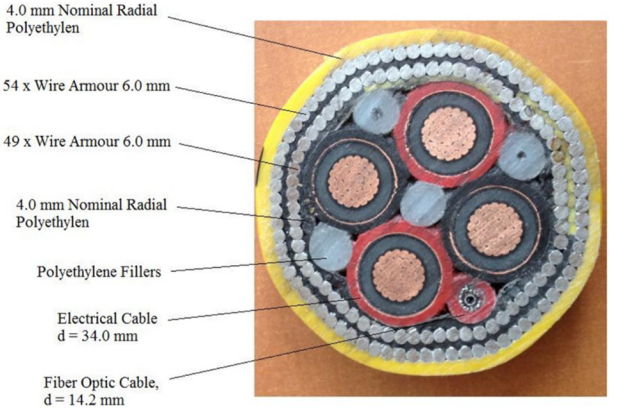

Figure 8.
Example of an actual high voltage cable with four copper wires

Source: Nguyen (2013)

The total diameter of the cable is 78 mm. The cable has four Cu wires with a diameter of 16.4 mm. The current density running through the Cu wires is equal to 1e6 A/m^2 (around 210 A) and is defined positively in two wires and negatively in the two others. A shield surrounds each wire to limit proximity effects and another one surrounds the four wires for a global shielding of the cable. Except for the conductors and shielding, the rest of the geometry is made of polyethylene terephthalate. The SE_H is studied at 1 cm from the high voltage cable.

In each application, the following equations are resolved:

$$\vec{\nabla} \times \vec{H} = \vec{J} \tag{1}$$

$$\vec{B} = \vec{\nabla} \times \vec{A} \tag{2}$$

$$\vec{E} = -\mathrm{j}\omega\vec{A} \tag{3}$$

$$\vec{J} = \sigma\vec{E} + \vec{J_e} \tag{4}$$

where $\vec{H}$ is the magnetic field, $\vec{B}$ is the magnetic induction, $\vec{A}$ is the magnetic vector potential, $\vec{E}$ is the electrical field, $\vec{J}$ is the total current density, $\vec{J_e}$ is the external current density, σ is the electrical conductivity and ω is the angular frequency. The imaginary unit j is defined by $\mathrm{j}^2 = -1$.

For the near-field application and the high voltage cable, the modelized system is bounded by a thick layer of infinite elements. The magnetic SE_H is then defined by:

$$SE_H = 20\log_{10}\frac{H_0}{H_{\text{shield}}} \tag{5}$$

with H_0 and H_{shield}, respectively, the magnetic field without and with the shield at the different observation points previously defined. SE_H is studied in each application at low frequencies from 1 Hz to 100 kHz.

The use of the 230 μm Al/steel/Al composite in these applications is compared to Al, steel and Cu in two cases, namely, first with equal thickness for applications with low space available and then with equal mass especially adapted for embedded applications. The following densities are used for calculations: 2.71 g/cm^3 for Al, 8.96 g/cm^3 for Cu, 7.85 g/cm^3 for steel and 3.57 g/cm^3 for the composite. Thus, the 230 μm Al/steel/Al composite is 2.5 and 2.2 times less dense than Cu and steel, but 1.3 times denser than Al. Materials properties considered into the numerical model for the magnetic shielding are summed up in Table II.

The numerical modeling of actual devices with the consideration of the heterogeneous layers of the composite is a real challenge regarding the scale differences from the material to the application. As a consequence, the composite material properties are here homogenized to

Table II. Relative permeability and conductivity of Cu, Al and steel

Material	Relative permeability μ	Conductivity σ, 10^6 S/m
Cu	1	59.98
Al	1	33.61
Steel	250	9.02

give reasonable computation time and memory consumption for the simulations. The principle of homogenization is shown in Figure 9. The properties of the equivalent layer are determined to obtain the same SE_H of the tri-layer composite.

In the case of the 230 μm composite, the determined equivalent properties are resumed in Table III. A slight difference is observed between RD and transverse direction (TD) properties. The presence of a few steel fractures considered in the homogenization process explains this difference. More details of the method to determine these properties by an energy approach can be found in a previous paper (Clérico *et al.*, 2019).

3. Results and discussions

3.1 Homogenization validation

Before comparing the SE_H of the composite with Al, Cu and steel, the homogenization method has to be validated by comparing the SE_H of the equivalent layer with the tri-layer one. The comparison between the tri-layer and the equivalent layer is shown in Figure 10 for the cylindrical box with the magnetic field observed at the vertical point.

The equivalent layer, with properties determined by homogenization, has an excellent concordance with the tri-layer. However, a slight difference can be seen for frequencies higher than 5 kHz. Indeed, the equivalent layer shows SE_H lower than the tri-layer with a maximal difference of approximately 4 dB.

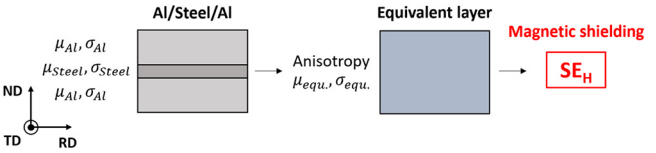

Figure 9.
Homogenization principle of the tri-layer composite

Table III.
Equivalent relative permeability and equivalent conductivity of a 230 μm Al/steel/Al composite

Direction	Relative permeability μ	Conductivity σ, 10^6 S/m
RD	41.61	29.507
TD	42.40	29.511
Normal direction	1.20	23.140

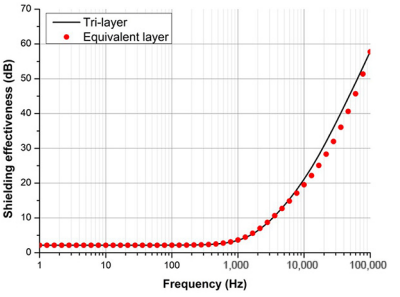

Figure 10.
SE_H of the tri-layer Al/steel/Al and its equivalent layer in the cylindrical box application (vertical point)

One parameter linked to the SE_H at high frequencies is the skin depth (Schelkunoff, 1943). Table IV gives the skin depth for Al, steel and the equivalent layer at different frequencies. As a reminder, the Al layer and steel layer thicknesses in the composite are, respectively, around 95.8 and 38.4 μm. Figure 11 shows the layer thickness divided by the skin depth as a function of frequency for Al, steel and the equivalent layer. The skin depth in Al is thicker than the layer thickness for all frequencies and, consequently, the magnetic field is very little absorbed by Al. The skin depth in steel attains the layer thickness at around 77 kHz. By definition (Schelkunoff, 1943), around 63 per cent of the magnetic field is then absorbed by steel at 77 kHz. The skin depth attains the equivalent layer thickness near 4 kHz. Thus, the equivalent layer absorbs better the magnetic field than the tri-layer composite. This difference in skin depth could explain the slight difference in SE_H at a frequency higher than 5 kHz.

3.2 Applications

The SE_H of the cylindrical box observed at the vertical and horizontal points are, respectively, presented in Figures 12 and 13. SE_H is calculated considering shields with equal thickness and equal mass. The results at these different points are almost similar. The SE_H is, nevertheless, a little higher at the vertical point than at the horizontal one.

As expected, Cu and Al do not shield low frequencies under 500 Hz due to their low relative magnetic permeability (close to 1). At higher frequencies, Cu shows better SE_H than Al with equal thickness because of its higher conductivity.

Frequency (Hz)	Skin depth (μm) Al	Steel	Equivalent layer
1	86,813	10,598	14,296
1,000	2,745	335	452
10,000	868	106	143
100,000	274	33.5	45.2

Table IV. Skin depth at different frequencies in Al, steel and the equivalent layer

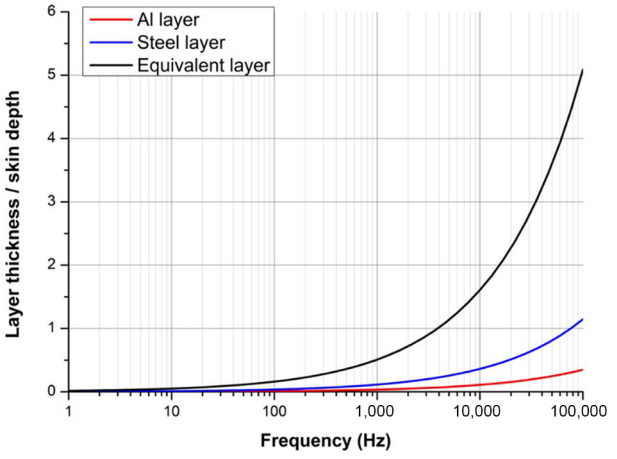

Figure 11. Layer thickness divided by the skin depth for Al, steel and the equivalent layer

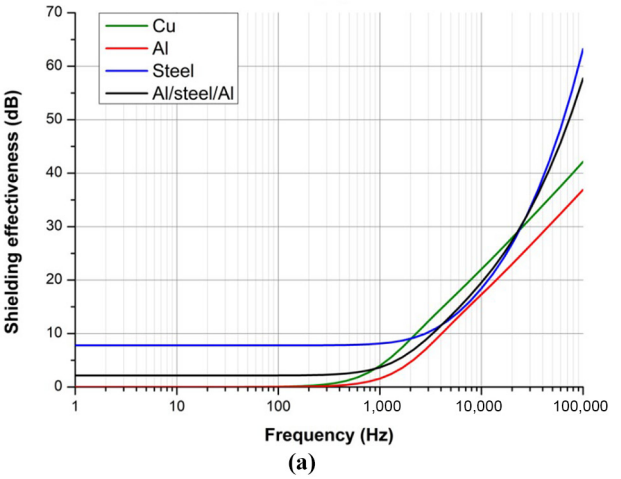

(a)

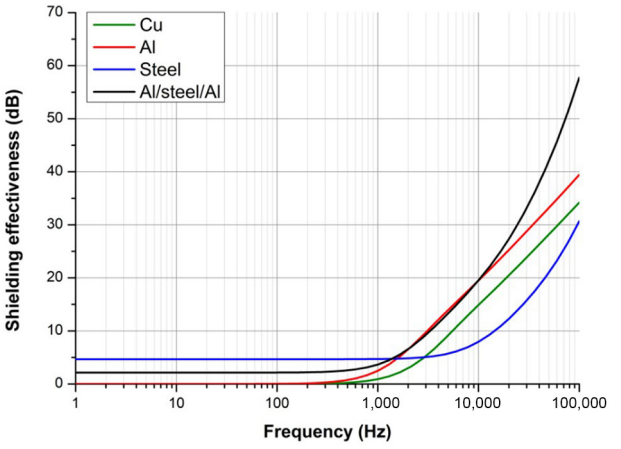

(b)

Figure 12.
SE_H of the cylindrical box with equal thickness (a) and equal mass (b) observed at the vertical point

Steel can shield low frequencies because of its high relative magnetic permeability. Furthermore, its increase in higher frequencies is steeper than the ones of Cu and Al. This steeper slope could be explained by a thinner skin depth in steel than in Cu and Al for a given frequency. Moreover, it can be noticed that the increase of the SE_H of steel begins at a higher frequency (ca. 2 kHz) than for Cu or Al (ca. 500 Hz) because of its smaller conductivity.

The composite can also shield low frequencies with a SE_H slightly lower than the steel one due to its lower relative magnetic permeability. In the equal thickness study, the SE_H of the composite is lower than the steel one on the entire frequency range. The use of the composite is then more beneficial at equal mass, its SE_H is greater than other ones at frequencies higher than 2 kHz.

Figures 14 and 15 introduce, respectively, the results of the equal thickness and equal mass studies for the squared box and the high voltage cable. The curves obtained are very similar to the cylindrical box ones. As previously, it is observed that the Al/steel/Al

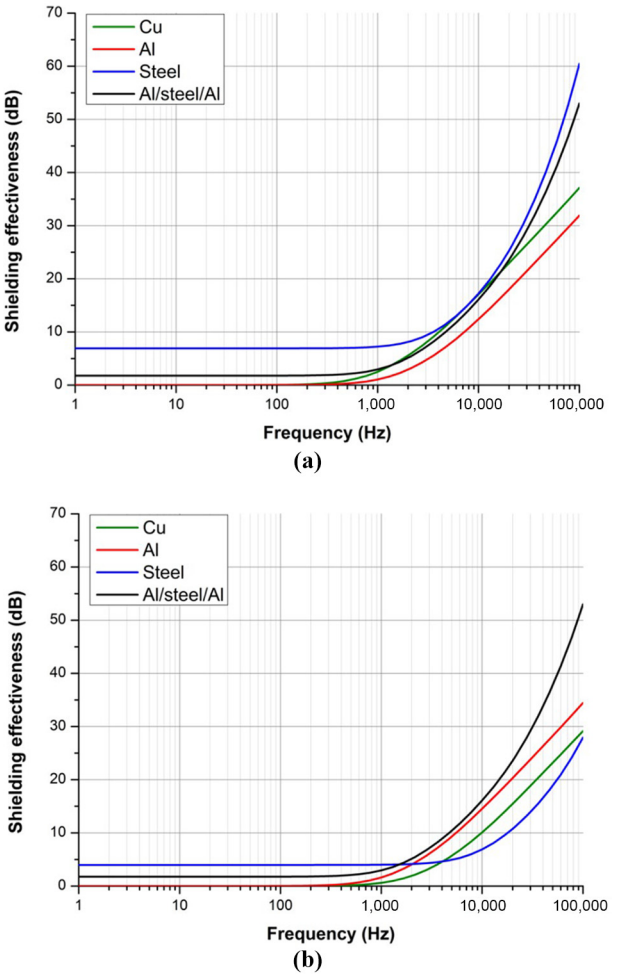

Figure 13.
SE_H of the cylindrical box with equal thickness (a) and equal mass (b) observed at the horizontal point

composite is more beneficial at equal mass and frequencies higher than (2-10 kHz). The composite could still be interesting at equal thickness. Indeed, its SE_H at high frequency is close to the steel one and can be higher than the Cu one with a lower density.

Figure 16 illustrates the comparison of the corresponding magnetic field distributions obtained at 1 Hz and 100 kHz for the aluminum, steel and composite solution at equal mass in the cable application. It is observed that at 1 Hz the use of steel and composite can significantly reduce the proximity effects. At 100 kHz, the composite shows a better effectiveness with magnetic field higher than 200 A/m confined within the first shield that surrounds each Cu wire.

To give some quantitative comparisons, Figure 17 resumes the results of the equal mass study for the three applications. The SE_H at 1 Hz, 1 kHz, 10 kHz and 100 kHz are drawn for the four studied materials. Cu has a SE_H a slightly lower than Al due to its higher density. Indeed, the SE_H of Cu and Al at 100 kHz is, respectively, around 37.8 and 43.2 dB in the far-

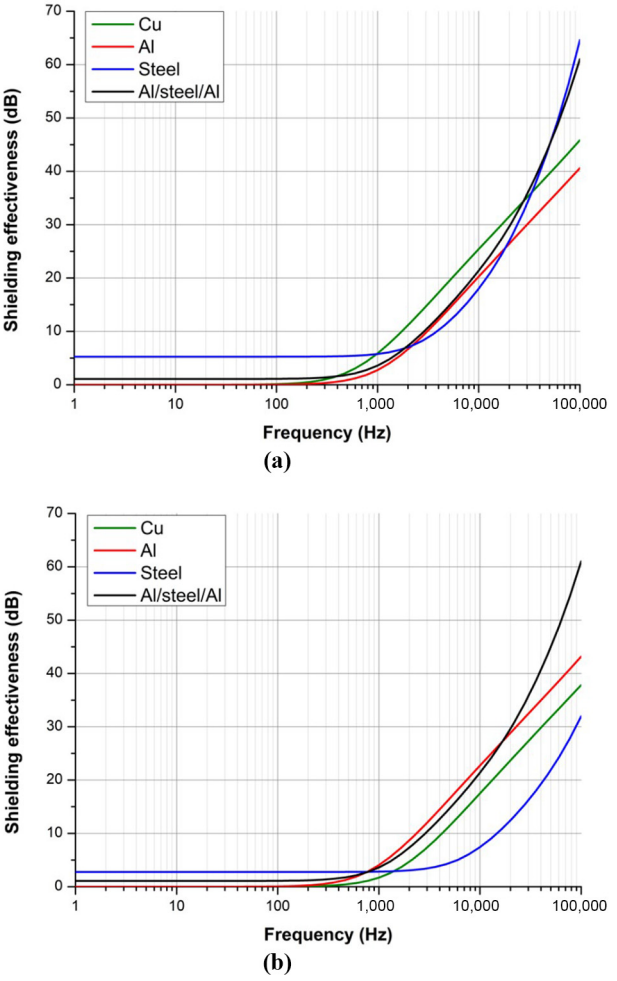

Figure 14.
SE_H of the squared box with equal thickness (a) and equal mass (b) observed at the central point

field application and 34.2 and 39.4 dB in the near-field application. Steel can shield low frequencies below (less than) 1 kHz but has lower SE_H at high frequency than Cu and Al: at 1 Hz and 100 kHz, respectively, 2.7 and 32 dB in the far-field application and 4.7 and 30.7 dB in the near-field application.

The SE_H obtained with the high voltage cable is greater than with the two previous applications, namely, at 100 kHz, SE_H of Cu, Al, steel and the composite is, respectively, 54.5, 65.4, 55.2 and 104.5 dB. The presence of several shields, one around each wire and another one around the four wires, explains this difference.

It is observed that, for each application, the homogenized composite is an interesting compromise at equal mass to shield low frequencies below 1 kHz and high frequencies above 10 kHz. In the case of the cylindrical box (near-field application), its SE_H at 1 Hz is around 2.1 dB, lower than that of steel, but better than that of Cu and Al. At 100 kHz, its SE_H is around 57.7 dB, better than Cu, Al and steel ones.

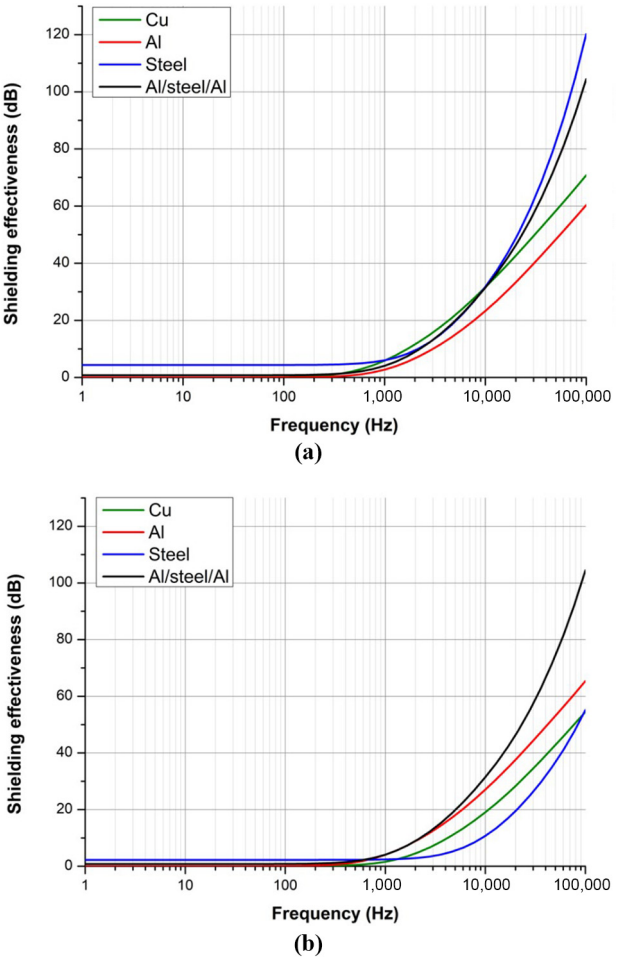

Figure 15.
SE_H of the high voltage cable with equal thickness (a) and equal mass (b) observed at 1 cm away from the cable

4. Conclusion

A composite constituted of a steel sheet sandwiched between two Al sheets has been successfully elaborated by CRB. The optimal trade-off between magnetic shielding and Al/steel interface adherence is obtained with a tri-layer composite of 230 μm. The homogenization method used to determine the material properties of an equivalent layer of this composite has been validated by the great agreement between the SE_H of the equivalent layer and the tri-layer one.

The SE_H of the 230 μm Al/steel/Al composite has then been studied in three applications with numerical simulations and compared to individual Cu, Al and steel layers. It has been shown that the Al/steel/Al composite is more beneficial at equal mass in each application. Indeed, the tri-layer composite can shield very low frequencies below 1 kHz and has SE_H at high frequencies above 10 kHz greater than Cu, Al and steel. Its SE_H at 1 Hz varies from 0.8 to 2.1 dB, depending on the application being modeled, compared to the steel shielding,

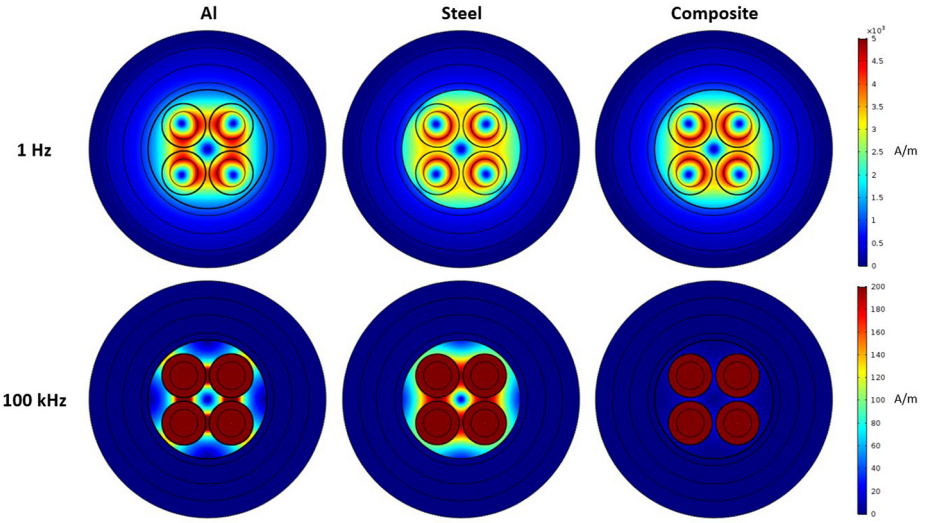

Figure 16.
Magnetic field distribution at 1 Hz and 100 kHz for the Al, steel and composite at equal mass in the cable application

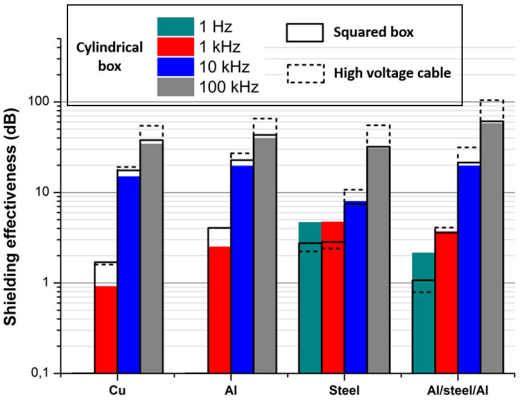

Figure 17.
SE_H of the cylindrical box, the squared box and the high voltage cable with different materials and frequencies at equal mass

which ranges from 2.2 to 4.7 dB. At 100 kHz, it varies between 57.7 and 104.5 dB compared to the Cu, Al and steel ones that vary, respectively, between 34.2 and 54.5 dB, 39.4 and 65.4 dB and 30.7 and 55.2 dB.

The study of the SE_H of the composite with more complex and realist geometry could be interesting. Thereby, the equivalent layer with homogenized properties can be used in the near future in three-dimensional models to reduce calculation and central processing unit time. This work can also be extended to other materials to increase the SE_H, especially at low frequency with material showing higher relative magnetic permeability.

References

Abdelli, W., Mininger, X., Pichon, L. and Trabelsi, H. (2012), "Impact of composite materials on the shielding effectiveness of enclosures", *Applied Computational Electromagnetic Society Journal*, Vol. 27 No. 4, pp. 369-375.

Ahn, S., Pak, J. and Song, T. (2010), "Low frequency electromagnetic field reduction techniques for the on-Line Electric Vehicle (OLEV)", *IEEE International Symposium on Electromagnetic Compatibility*, pp. 625-630.

Al-Ghamdi, A.A., Al-Hartomy, O.A., El-Tantalwy, F. and Yakuphanoglu, F. (2015), "Novel polyvinyl alcohol/silver hybrid nanocomposites for high performance electromagnetic wave shielding effectiveness", *Microsystem Technologies*, Vol. 21 No. 4, pp. 859-868.

Chung, D.D. (2001), "Electromagnetic interference shielding effectiveness of carbon materials", *Carbon*, Vol. 39 No. 2, pp. 279-285.

Clérico, P., Mininger, X., Prévond, L., Baudin, T. and Helbert, A.-L. (2019), "Compromise between magnetic shielding and mechanical strength of thin Al/steel/Al sandwiches produced by cold roll bonding: experimental and numerical approaches", *Journal of Alloys and Compounds*, Vol. 798, pp. 67-81.

Dawson, T.W., Caputa, K., Stuchly, M.A., Sphaphard, R.B., Kavet, R. and Sastre, A. (2002), "Pacemaker interference by magnetic fields at power line frequencies", *IEEE Transactions on Biomedical Engineering*, Vol. 49 No. 3, pp. 254-262.

Kim, D.H., Kim, Y. and Kim, J.W. (2016), "Transparent and flexible film for shielding electromagnetic interference", *Materials and Design*, Vol. 89, pp. 703-707.

Li, M.Z., Jia, L.C., Zhang, X.P., Yan, D.X., Zhang, Q.C. and Li, Z.M. (2018), "Robust carbon nanotube foam for efficient electromagnetic interference and microwave absorption", *Journal of Colloid and Interface Science*, Vol. 530, pp. 113-119.

Liu, X., Wu, J., He, J. and Zhang, L. (2017), "Electromagnetic interference shielding effectiveness of titanium carbide sheets", *Materials Letters*, Vol. 205, pp. 261-263.

Ma, X., Zhang, Q., Luo, Z., Lin, X. and Wu, G. (2016), "A novel structure of Ferro-Aluminum based sandwich composite for magnetic and electromagnetic interference shielding", *Materials and Design*, Vol. 89, pp. 71-77.

Nguyen, D.Q. (2013), "Développement d'un outil d'investigation pour le diagnostic des phénomènes hautes fréquences dans les câbles électriques", PhD thesis, École Nationale Supérieure d'Arts et Métiers.

Ray, M., George, J.J., Chakraborty, A. and Bhowmick, A.K. (2010), "An investigation of the electromagnetic shielding effectiveness of ethylene vinyl acetate elastomer reinforced with carbon nanofillers", *Polymers and Polymer Composites*, Vol. 18 No. 2, pp. 59-65.

Schelkunoff, S.A. (1943), "Electromagnetic waves", Bell Telephone Laboratories series, Van Nostrand.

Smolenski, R., Bojarski, J., Kempski, A. and Lezynski, P. (2014), "Time-domain-based assessment of data transmission error probability in smart grids with electromagnetic interference", *IEEE Transactions on Industrial Electronics*, Vol. 61 No. 4, pp. 1882-1890.

Xu, Z. and Hao, H. (2014), "Electromagnetic interference shielding effectiveness of aluminum foams with different porosity", *Journal of Alloys and Compounds*, Vol. 617, pp. 207-213.

Corresponding author
Paul Clérico can be contacted at: Paul070692@aol.com